

Simulation and quantification of performance of roadway systems using geogrid reinforcements

Sangy Hanumasagar

Advisor: Prof. J. David Frost

Sustainable Geotechnical Systems Laboratory

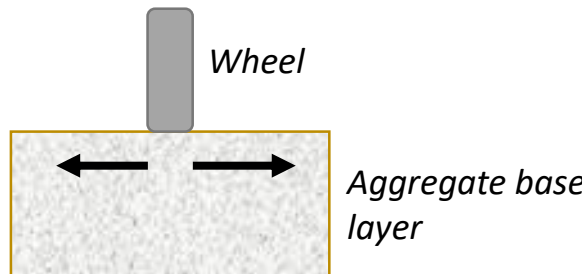
12 June 2019

Outline

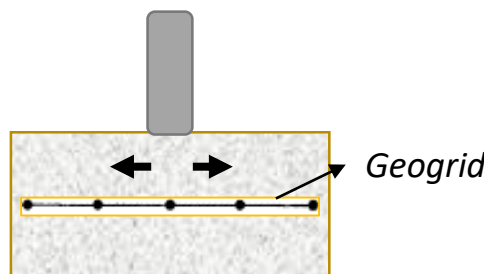
- **Introduction**
- **Bench-scale Pavement Testing**
- **Experimental Simulations** [data collection, preliminary observations, hypotheses formulations]
- **Computational Simulations** [simulation validation tests, comparison of results with experimental data, data mining, validation of hypotheses]
- **Future Work and Conclusions**

Introduction: Motivation and Background

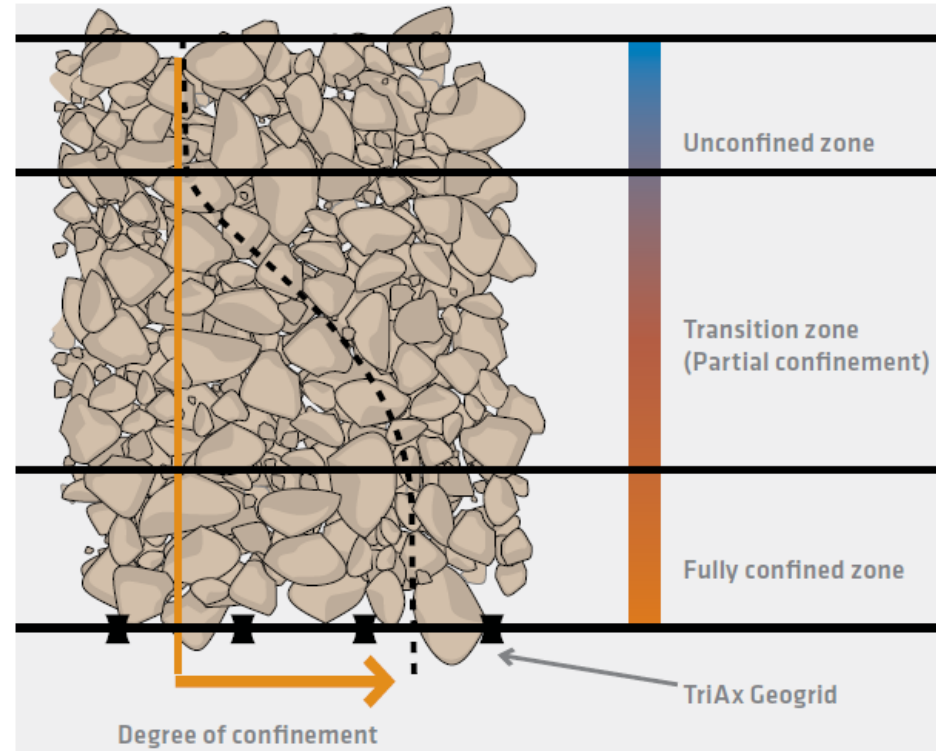
Understanding fundamental aggregate-geogrid interaction



Lateral spreading of particles



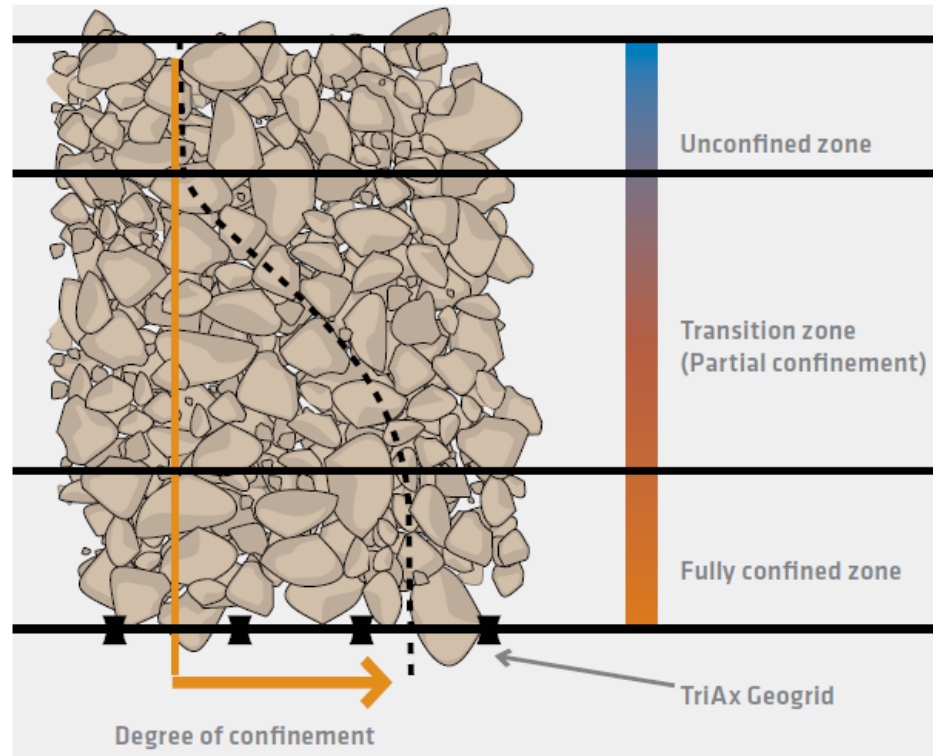
Reduced spreading by
interlocking with geogrid



Confinement induced by aggregate-geogrid interlocking
(Tensar Subgrade Stabilization Manual)

Introduction: Motivation and Background

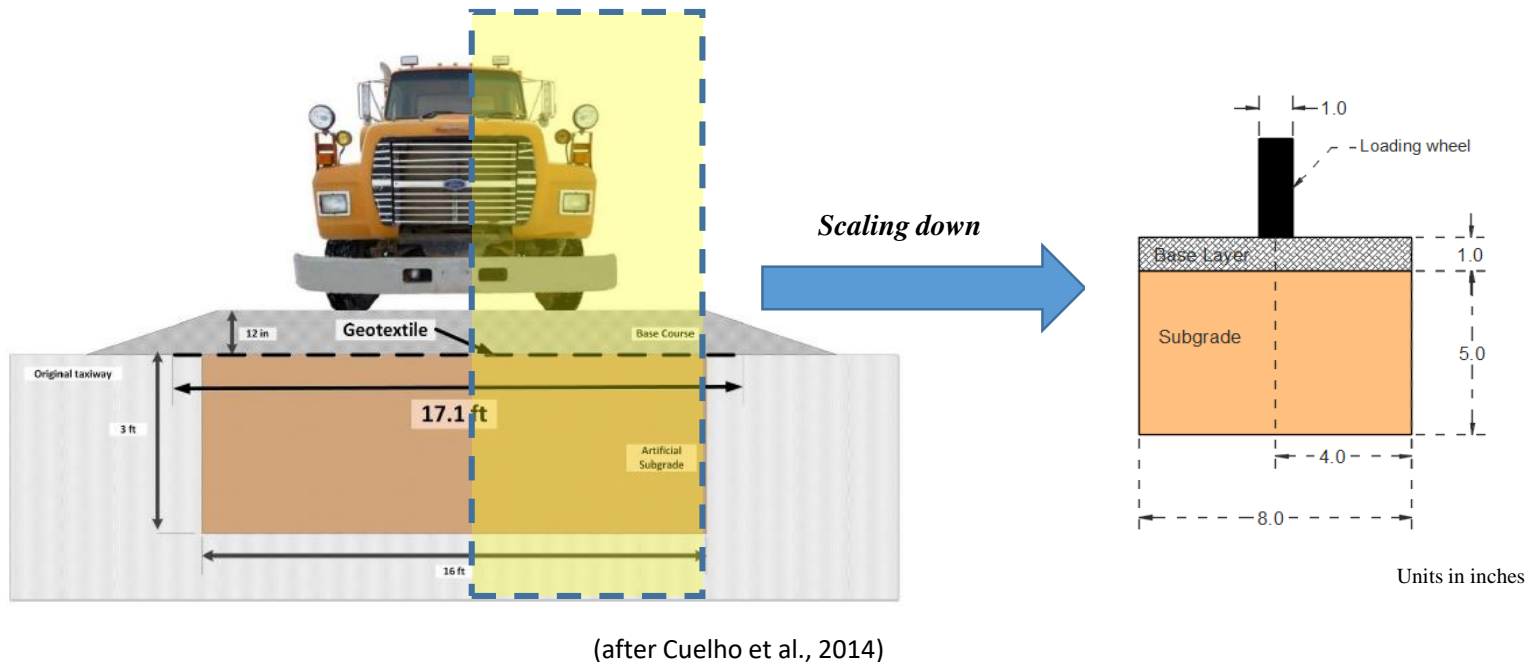
- How do we maximize interlocking?
 - Grid location
 - Aggregate-Geogrid Compatibility
 - Aggregate properties
- How do we measure it?



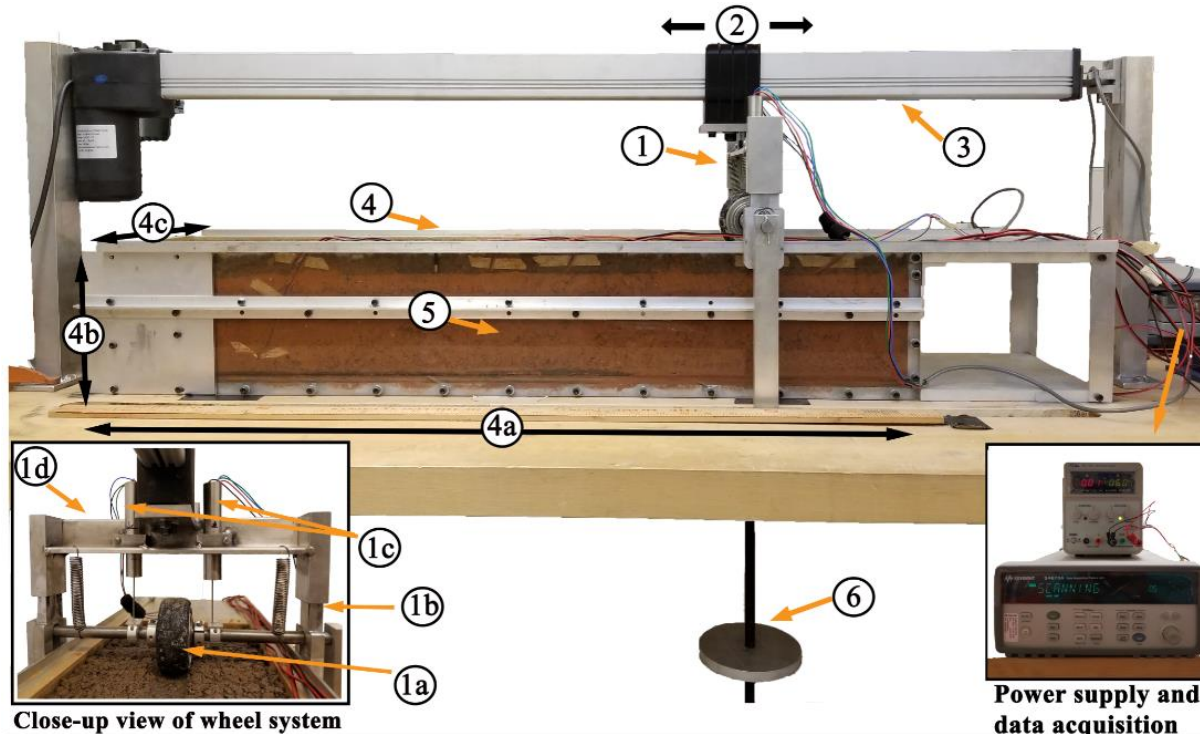
Confinement induced by aggregate-geogrid interlocking
(Tensar Subgrade Stabilization Manual)

Introduction: Motivation and Background

Schematic showing cross-sections of full-scale and bench-scale specimens

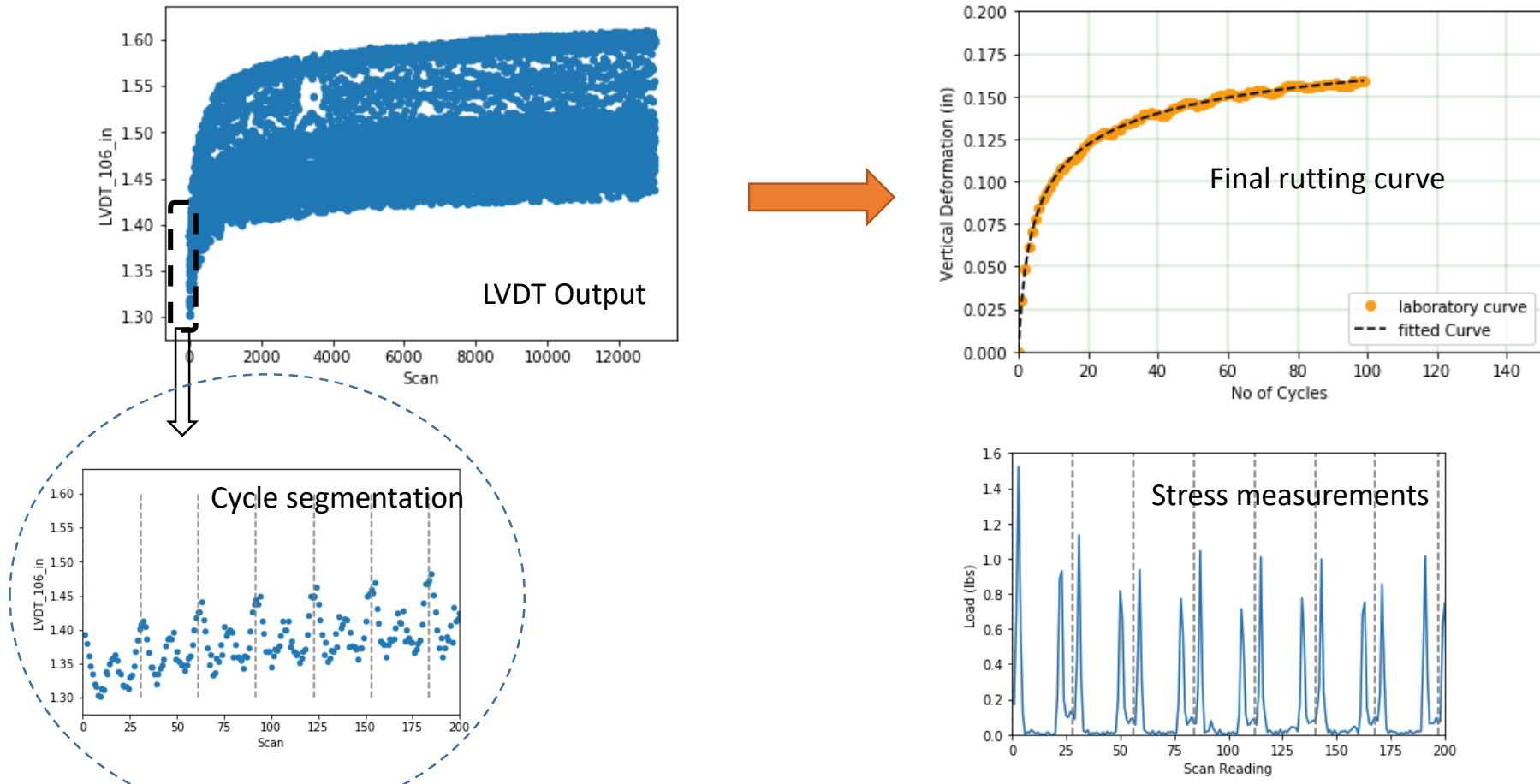


Bench-scale Pavement Testing Setup



- | | | |
|---|--|--|
| 1) Wheel system
a) Wheel (3 in Ø, 1 in width)
b) Adjustable yoke
c) Linear variable displacement transducers
d) Support frame | 2) Direction of wheel motion
3) Micro-conroller driven track actuator
4) Box
a) 36 in length
b) 6 in height
c) 8 in width | 5) Transparent lexan wall
6) Suspended loading system |
|---|--|--|

Bench-scale Pavement Testing Setup



Experimental Study

Effect of Aggregate Morphology on Rutting Behavior

Material Properties

Aggregate Samples

RA Material
Pea Gravel
Sub-rounded and smooth



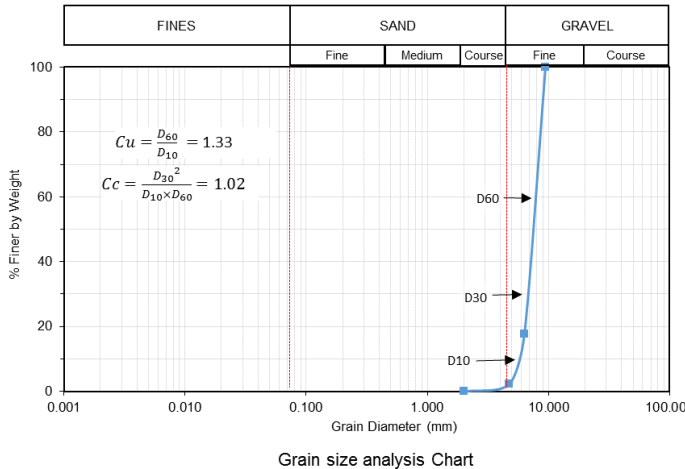
QA Material
#89 Stone
Angular and rough



Steel Grids (SG)

Steel Grid	Aperture Size, in. (mm)	Rib Thickness, in. (mm)
SG1	0.25 (6.35)	0.020 (0.50)
SG2	0.50 (12.7)	0.032 (0.815)
SG3	0.75 (19.05)	0.069 (1.76)
SG4	1.00 (25.4)	0.055 (1.4)

Grain Size Distribution

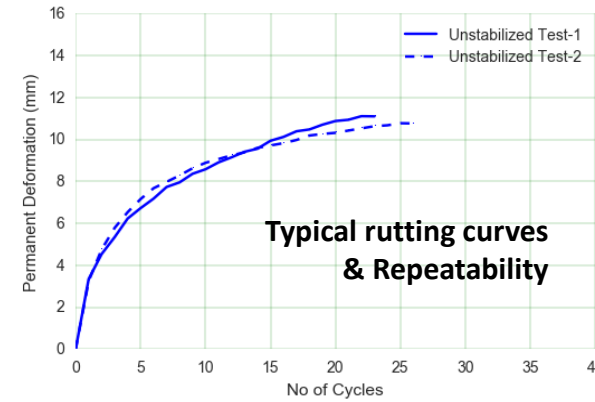
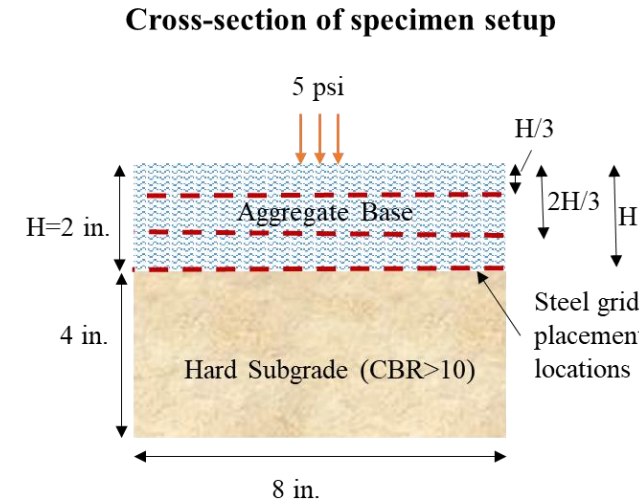


Experimental Program

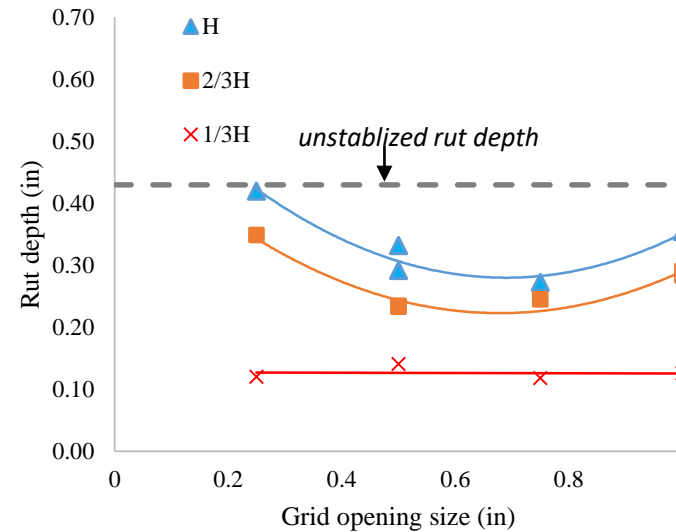
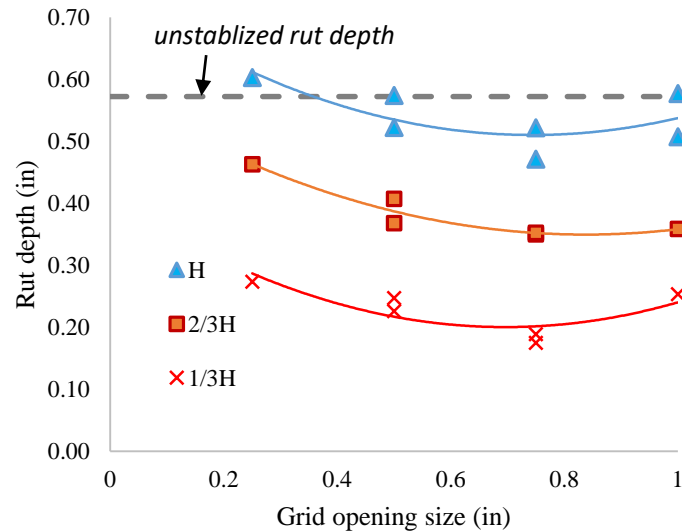
- Loading stress = 5 psi (35 kPa)
- Loading Duration = 35 cycles
- Testing Program
 - 2 aggregates
 - 4 scenarios of stabilization using each grid



Typical rut formations



Results and Discussion



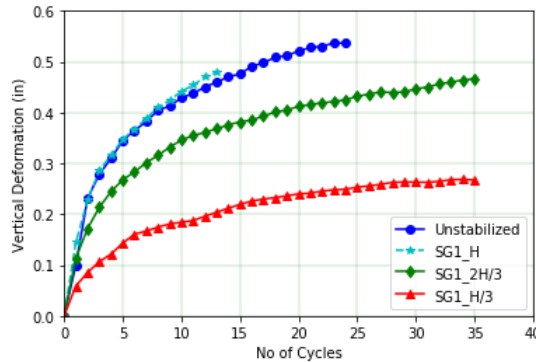
Rutting depth for (a) RA and (b) QA materials and all four grid openings

Results and Discussion

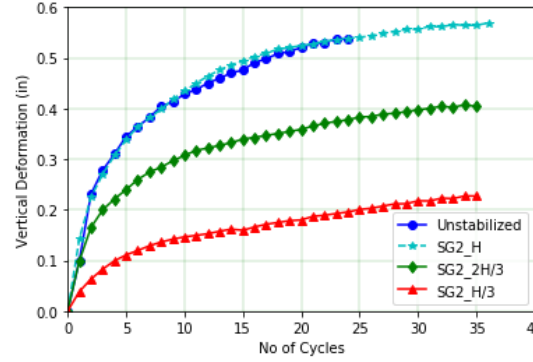
RA Aggregate: Rutting behavior for various stabilization scenarios



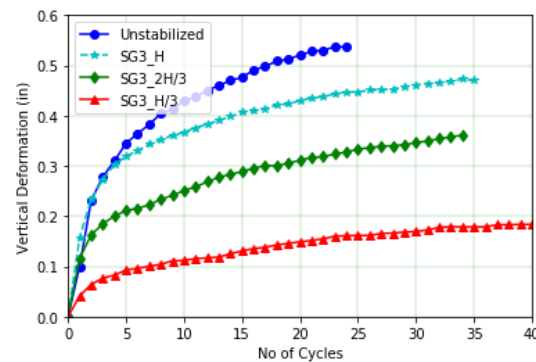
SG1 – ¼ in. opening size



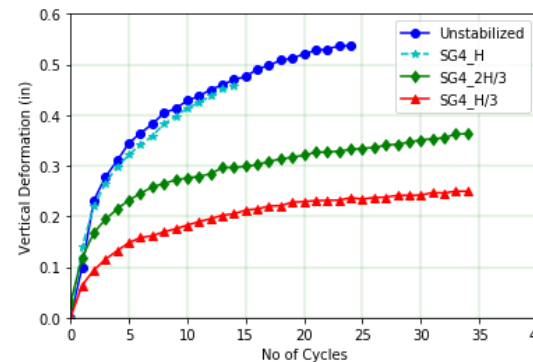
SG2 – ½ in. opening size



SG3 – ¾ in. opening size

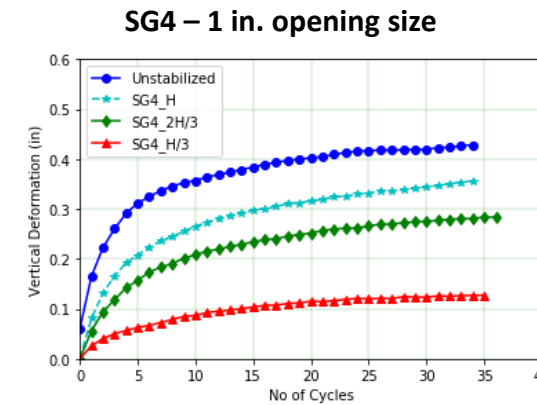
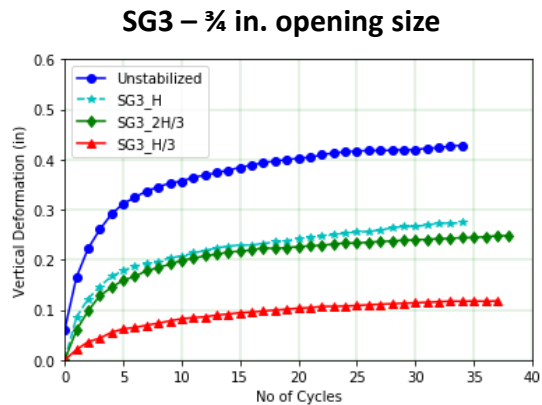
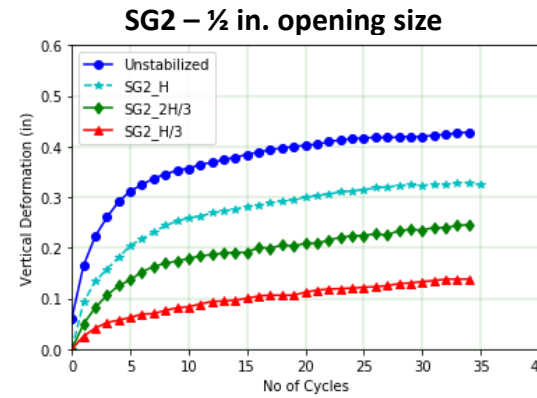
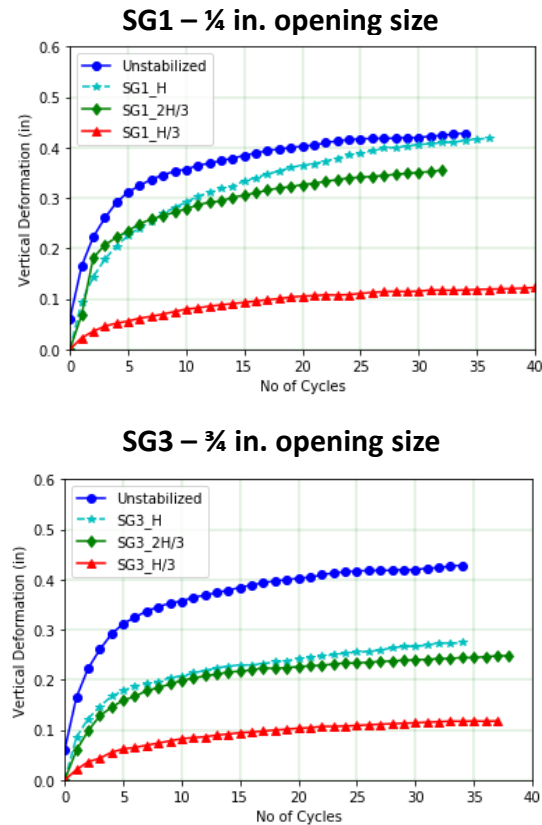


SG4 – 1 in. opening size



Results and Discussion

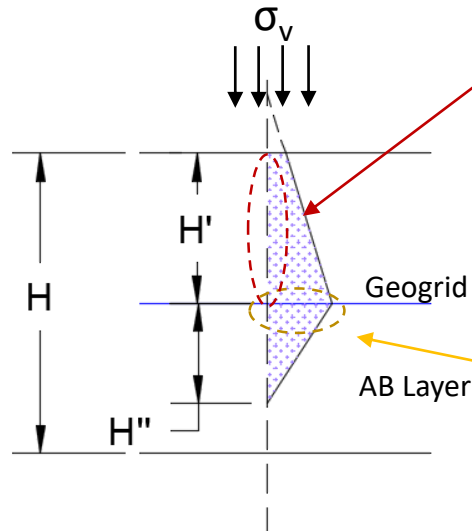
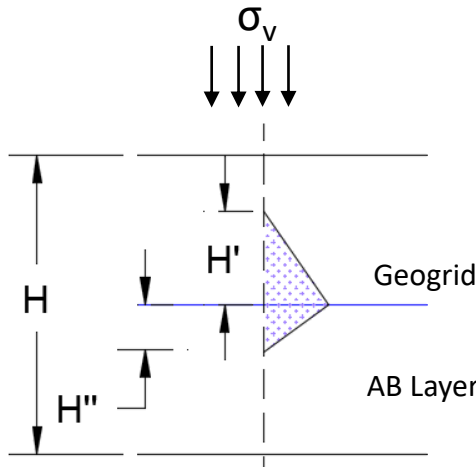
QA Aggregate: Rutting behavior for various stabilization scenarios



Results and Discussion

- QA showed consistent reduction in rutting while RA only showed change for shallow grid placement
- QA is more bilinear than RA

$$GG \text{ performance} \sim f(\sigma_v, H', b)$$



Effect of aggregate morphology on rutting behavior, H'

Aggregate-geogrid compatibility, b

Hypothetical zones of confinement induced by geogrid

Computational Study

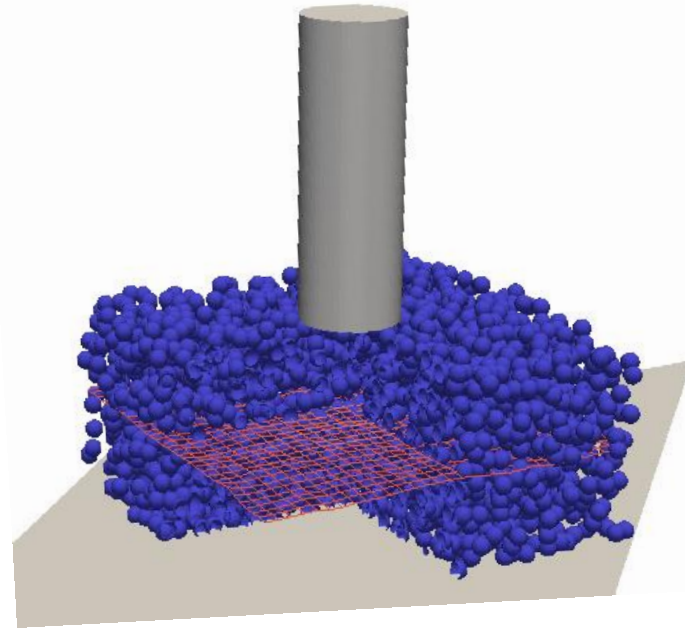
Aggregate-Geogrid Interaction

Objectives of Simulation Study

- Understanding the influence of following parameters on aggregate-geogrid interaction:
 - **Loading stress** [70, 100, 140, 190 kPa]
 - **Aggregate to geogrid ratio** [12.5 mm particles with 12.5, 25, 37, 60 mm GG]
 - **Depth of geogrid installation** [0.3H vs 0.5H from surface]
 - **Aggregate properties** (no rolling resistance vs with rolling resistance)
 - **Grid properties** (geogrid vs steel)
- Identify aggregate-geogrid interaction zone to highlight stabilization effects of different aggregate-geogrid combinations

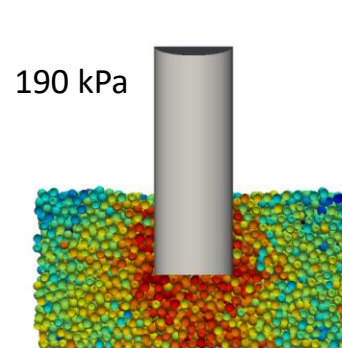
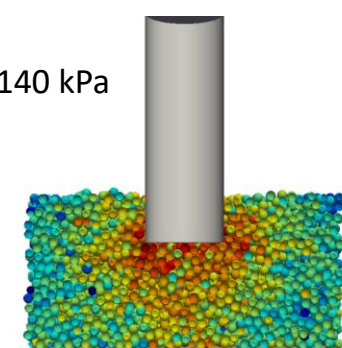
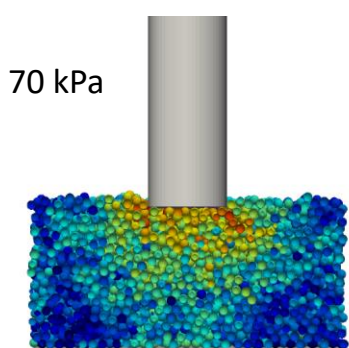
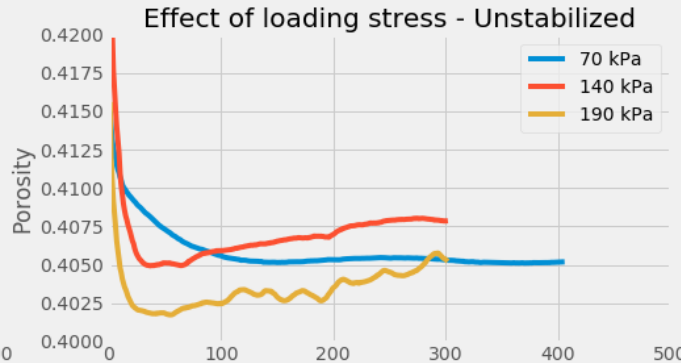
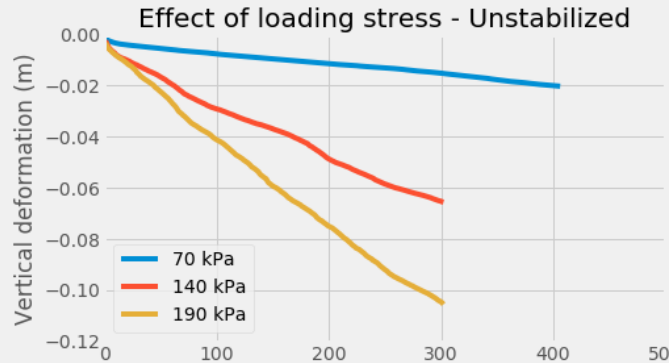
Simulation Hyper parameters

Auxiliary variables	Value range
Chamber dimensions	0.4 x 0.4 m
Specimen thickness	0.2 m (post-densification)
Loading cylinder diameter	0.1 m
Damping	0.7
Particle variables	Value range
Diameter	12.5 mm
Density	2700 kg/m ³
Friction angle	45
Geogrid variables	Value range
Rib thickness	1.27 mm
Young's Modulus	0.2 m (post-densification)
Rib stiffness	220 kN/m
Flex stiffness	scaled to bend to 41.5° for same length of geogrid



Simulation setup

Effect of stress: 70, 140 & 190 kPa [Unstabilized]

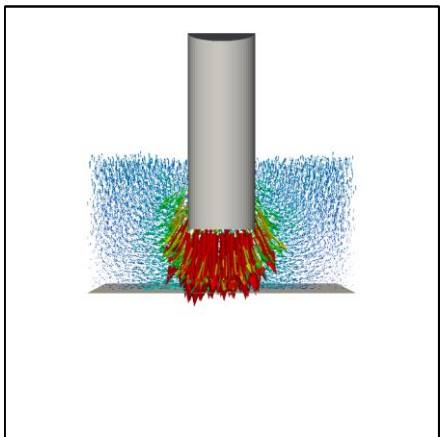


Observations from porosity

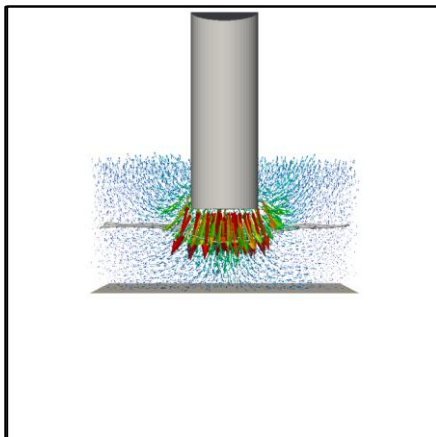
- 140kPa specimen had higher initial porosity than other two [0.415, 0.426, 0.415]
- Drastic densification followed by dilation at higher stresses

Profiles of simulation system after 300 loading cycles (colors indicate particle rotation)

Effect of GG: Unstabilized vs Stabilized [25 mm biaxial GG, 190 kPa]

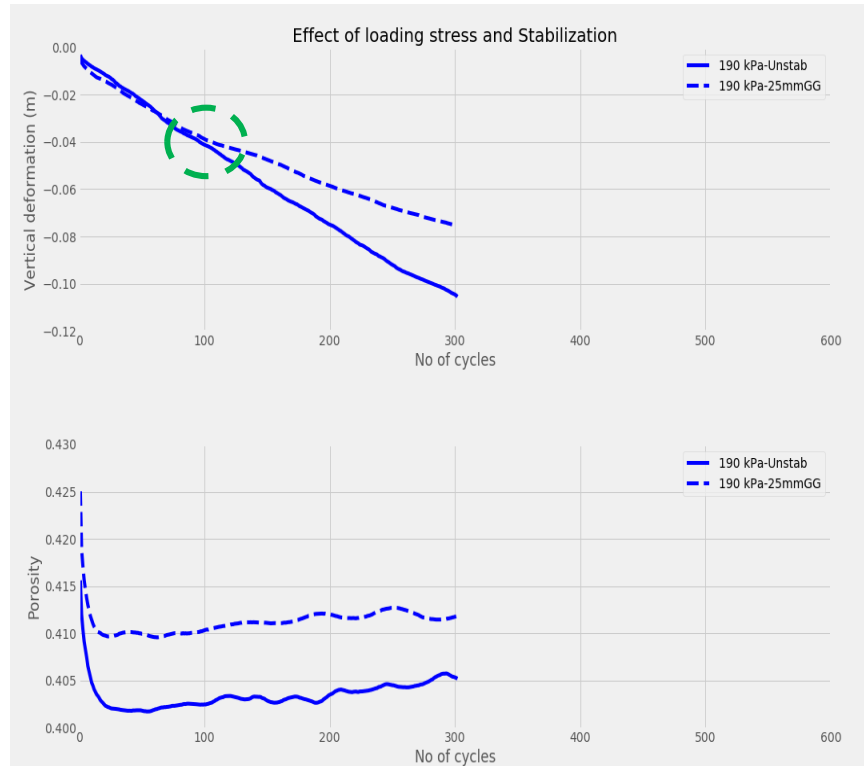


Unstabilized



[Stabilized- 25 mm GG
GG location = $H/2$ from base

Cycle 300

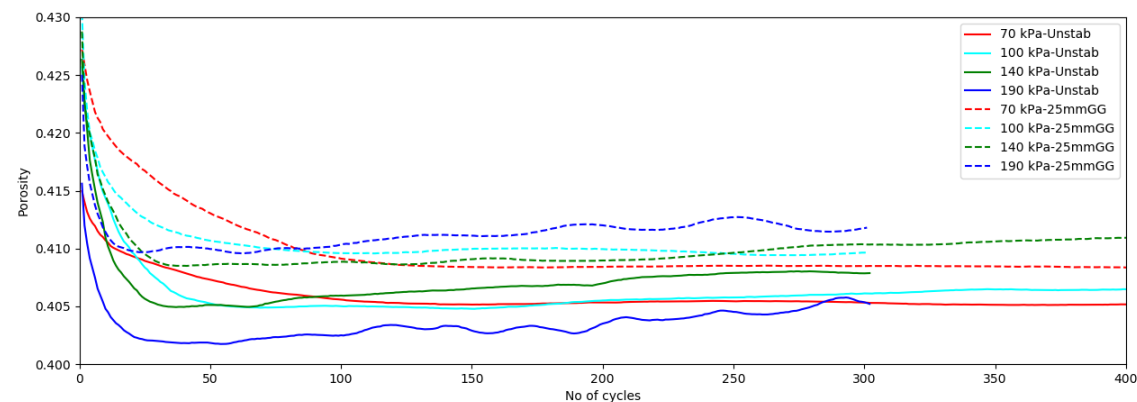
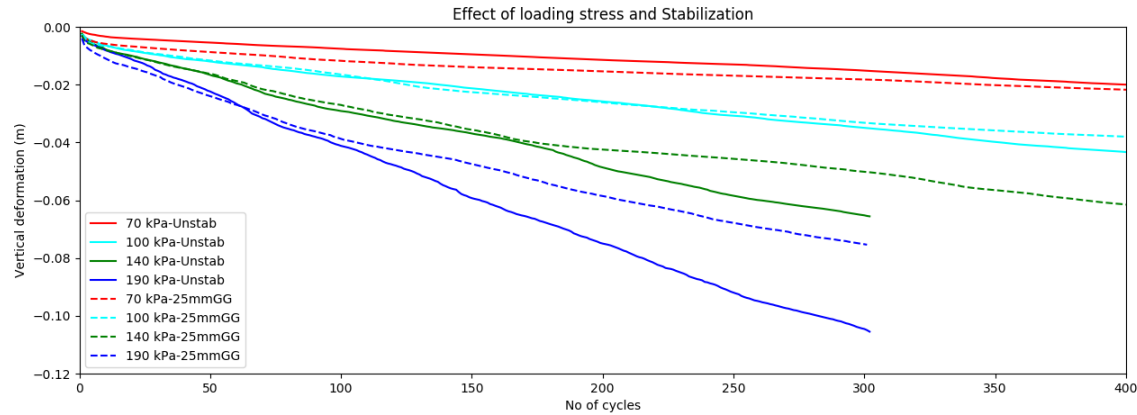


Observations

- GG influence is observed at 90 cycles \rightarrow start of interaction zone
- Distance of loading cylinder to GG = interaction zone thickness?

Surface rutting and porosity curves

Effect of stress:70, 100, 140, 190 kPa [Unstab and 25 mm GG]



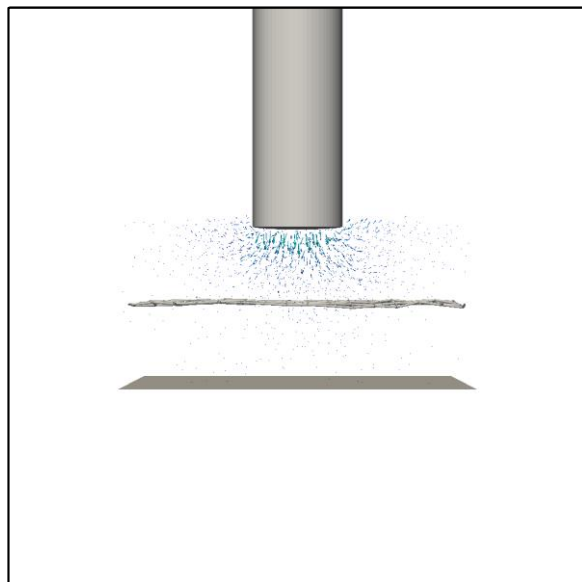
Observations

- Rutting curves for unstabilized & stabilized cases deviate from each other at different stages of test-
 - 70kPa – Identical throughout
 - 140 kPa- shift at 180 cycles
 - 190 kPa – shift at 90 cycles
- At 70 kPa, the lateral disp front does not even reach the geogrid height

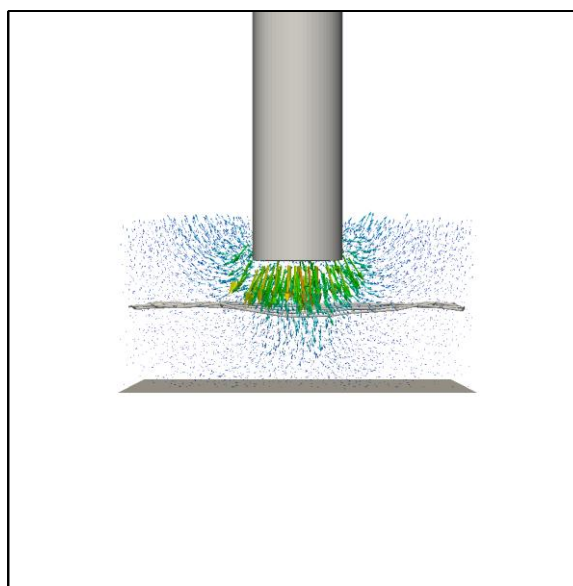
Surface rutting and porosity curves

Effect of stress:70, 140, 190 kPa [25 mm GG]

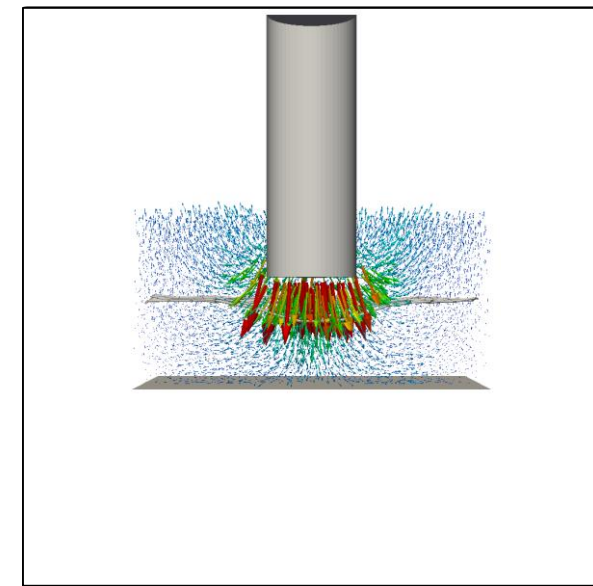
Cycle 300



Stabilized- 25 mm GG
70 kPa



Stabilized- 25 mm GG
140 kPa

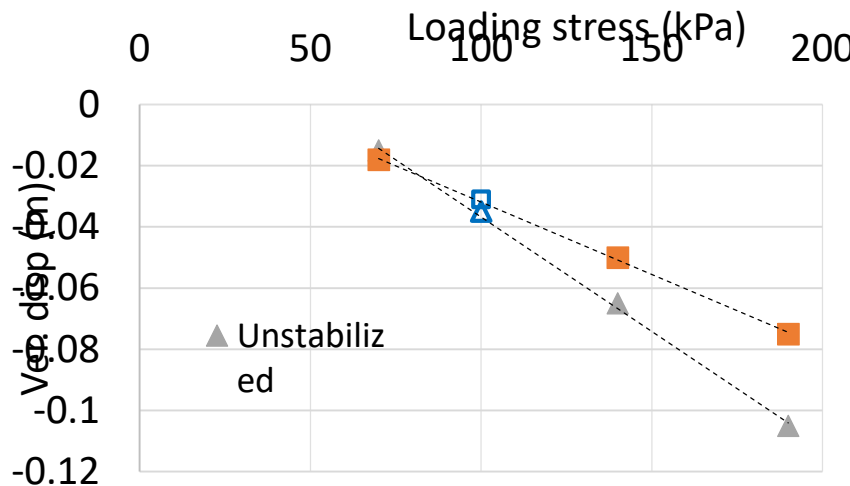


Stabilized- 25 mm GG
190 kPa

Rut Reduction at various stresses

Observations

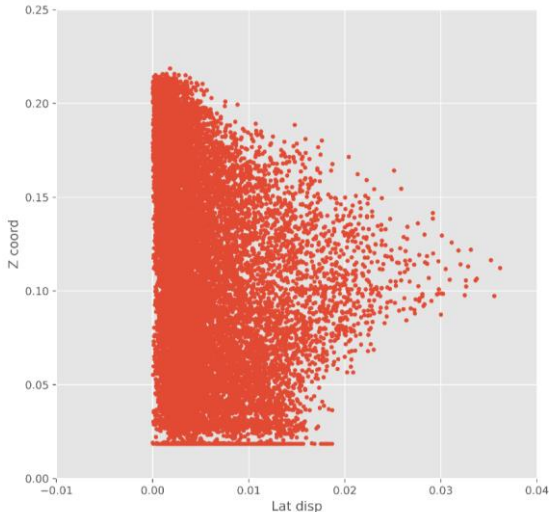
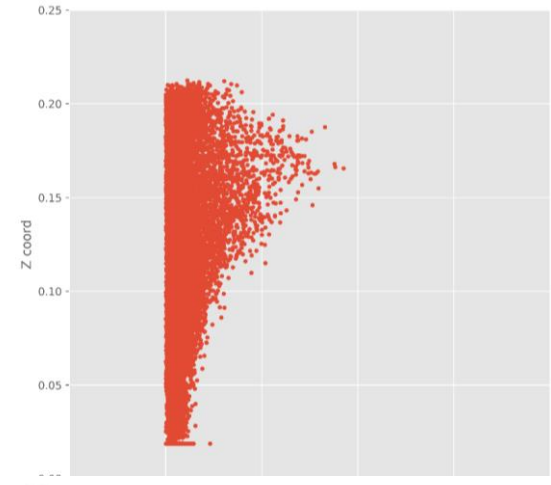
- Greater influence of geogrid as pavement is distressed more



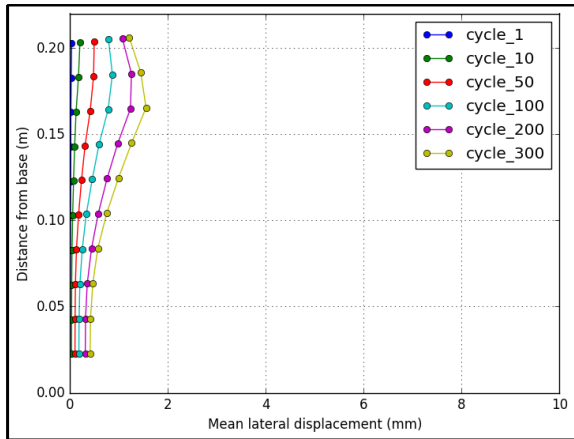
Influence of geogrid at various stress levels

Lateral spreading at 100 kPa at 300 cycles

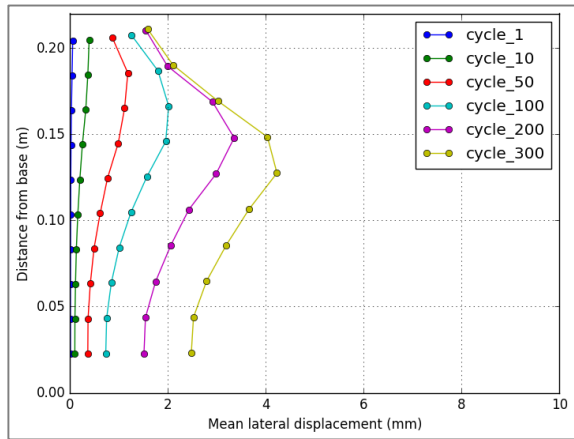
Lateral spreading at 190 kPa at 300 cycles



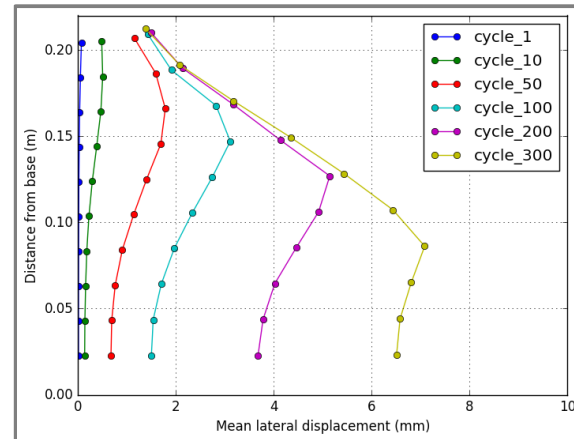
Effect of stress: 70, 140 & 190 kPa [Unstabilized]



Unstabilized
70 kPa



Unstabilized
140 kPa



Unstabilized
190 KPa

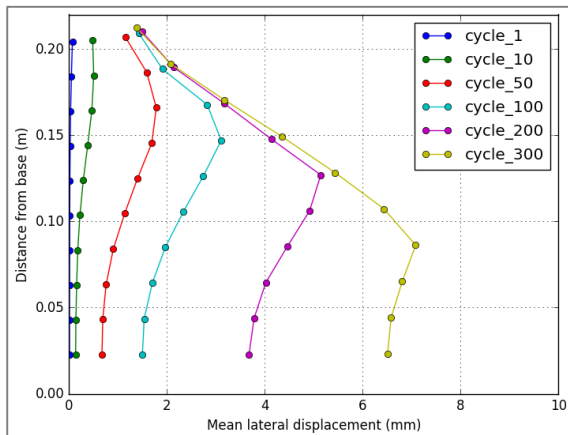
Profiles of **mean lateral displacement** across thickness of aggregate layer at various testing stages

Notes:

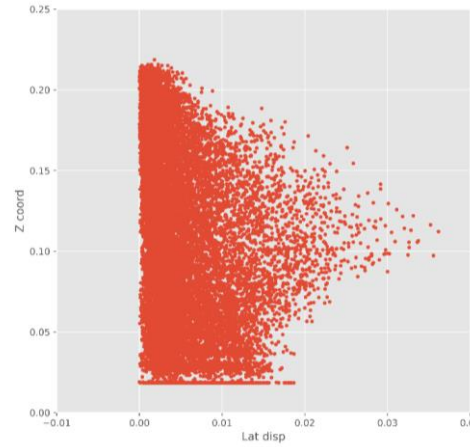
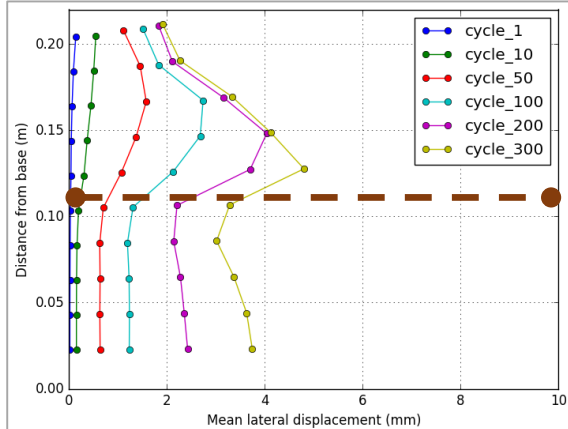
- **Mean lateral displacement** is calculated as average of lateral displacements of all particles in each sub-layer (totally 10 sub layers)
- Progressive downward movement of point of maximum lateral displacement with increasing loading cycles

Lateral Disp Profiles : Unstab vs Stab [190 kPa]

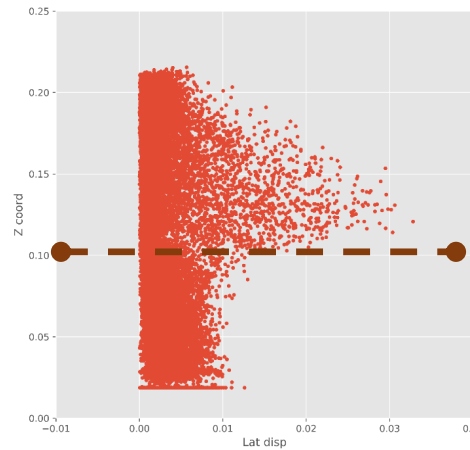
Unstabilized at
190 KPa



Stabilized- 25
mm GG at 190
KPa

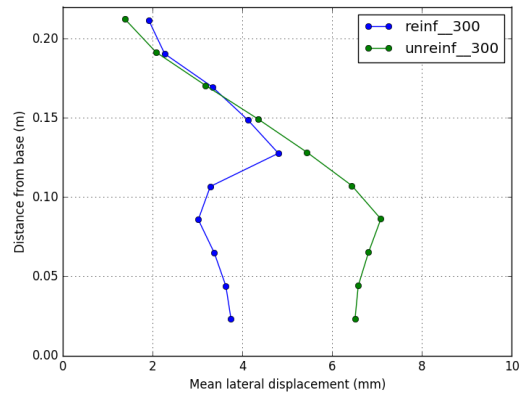
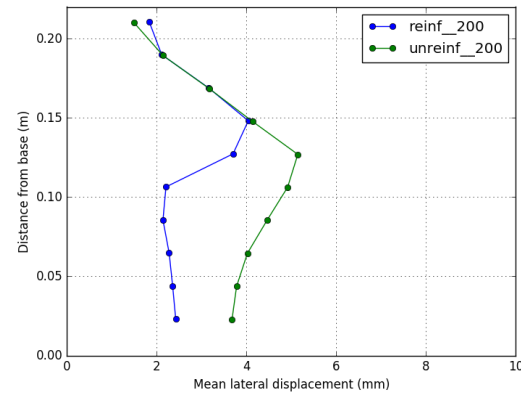
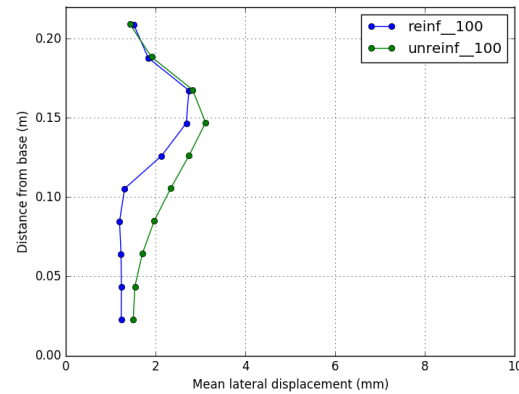
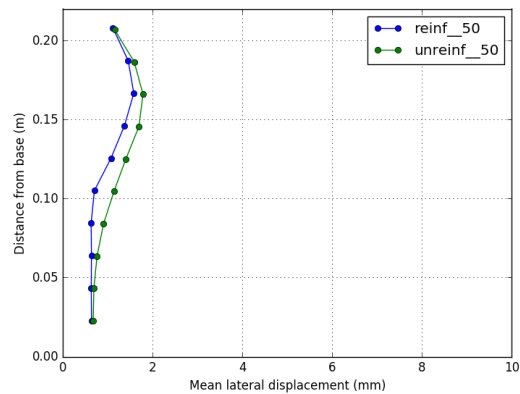
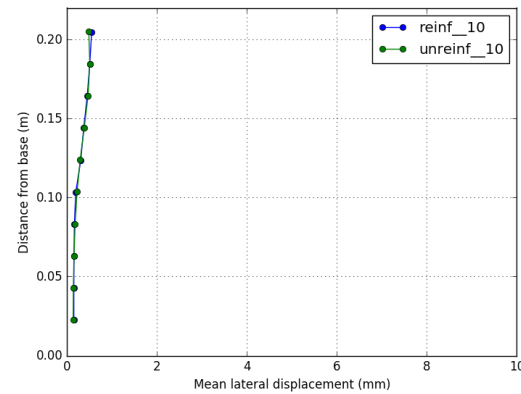
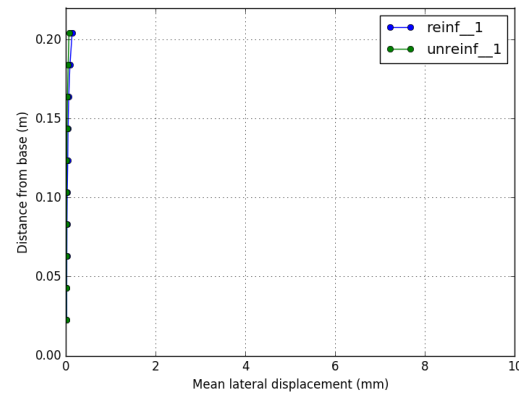


Lateral spreading
without geogrid at
300 cycles



Lateral spreading
with geogrid at 300
cycles

Geogrid Influence Zone – 25 mm GG

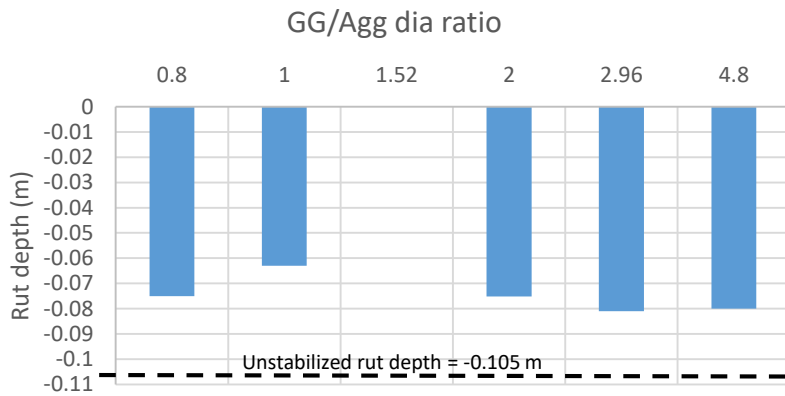


Comparison mean lateral displacement profiles for Unstabilized & 25mm-GG stabilized specimens

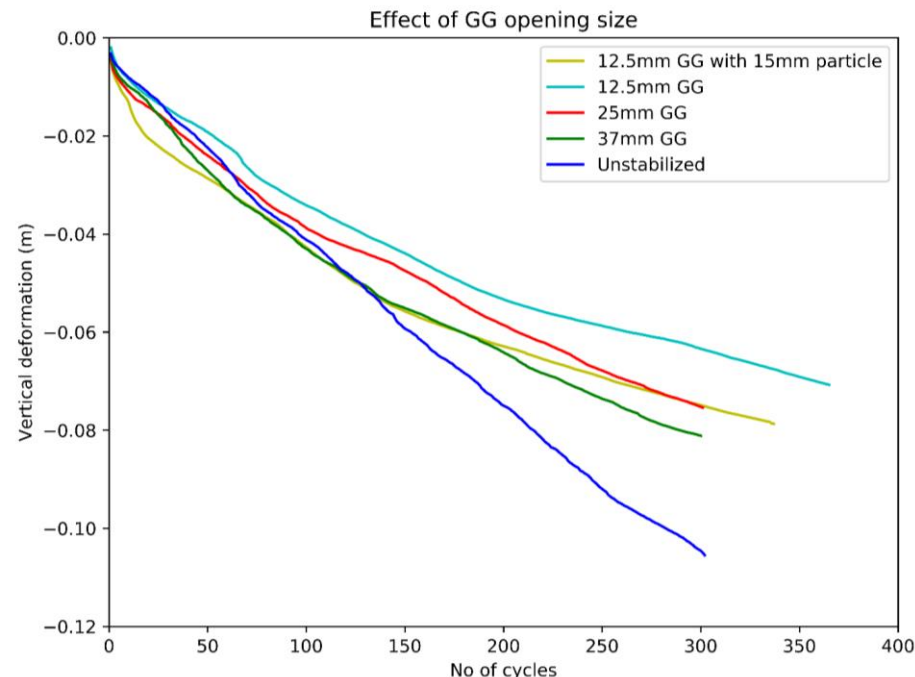
Effect of GG opening size: 12.5, 25.4, 37, 60 mm [190 kPa]

Observations

- 12.5 mm GG shows lowest rutting
- 37mm and 60mm rutting curves as well as lateral displacement curves (2 slides down) are identical



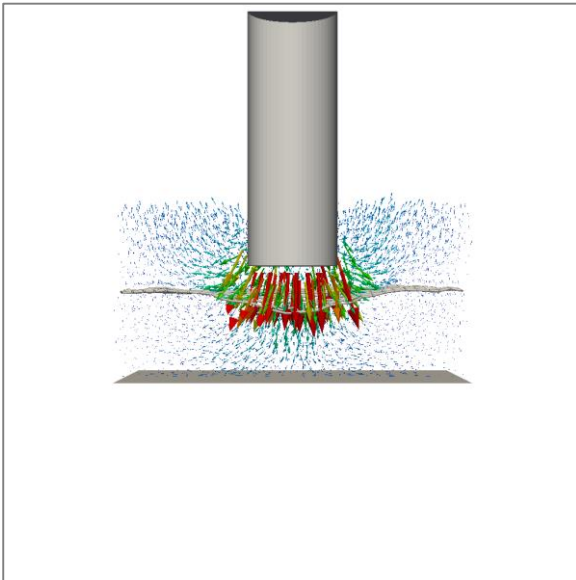
Geogrid to aggregate diameter ratio vs rut depth



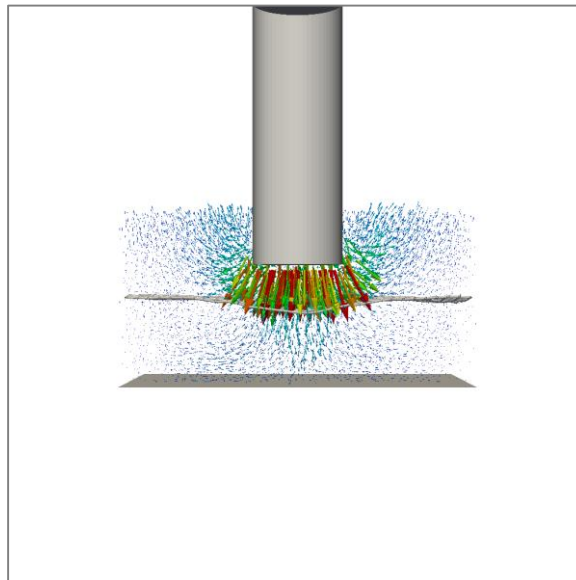
Surface rutting curves using various geogrids

Effect of GG opening size

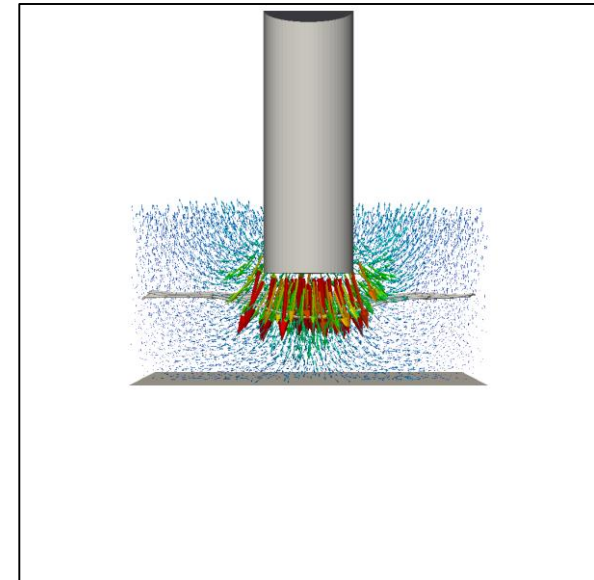
Cycle 300



Stabilized- 12.5 mm GG, 15 mm agg

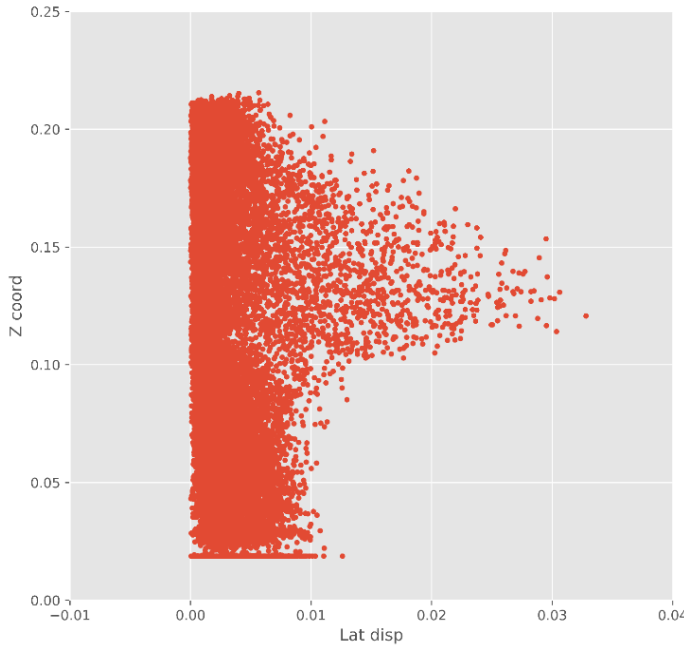


Stabilized- 12.5 mm GG, 12.5 mm agg

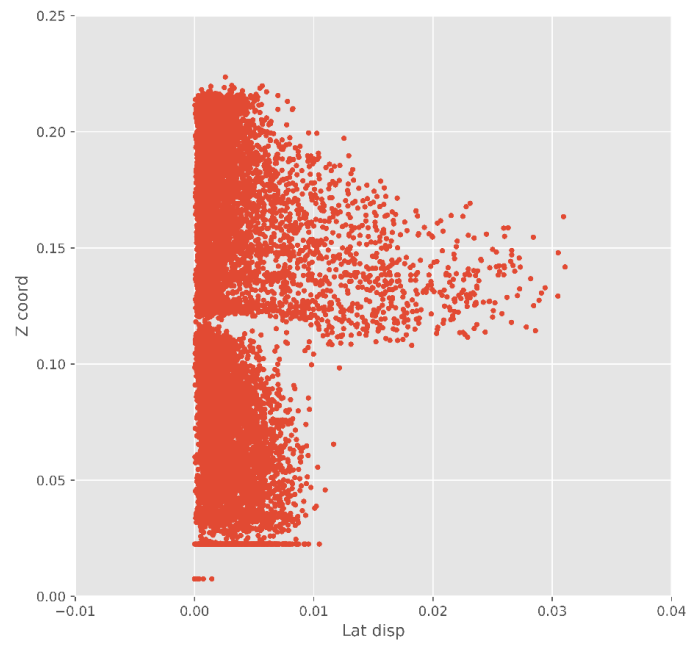


Stabilized- 25 mm GG, , 12.5 mm agg

Evidence for lack of interlocking

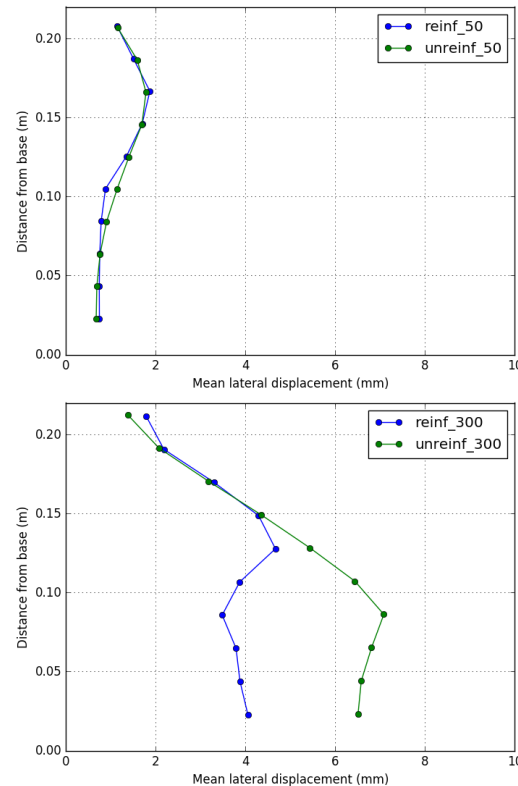
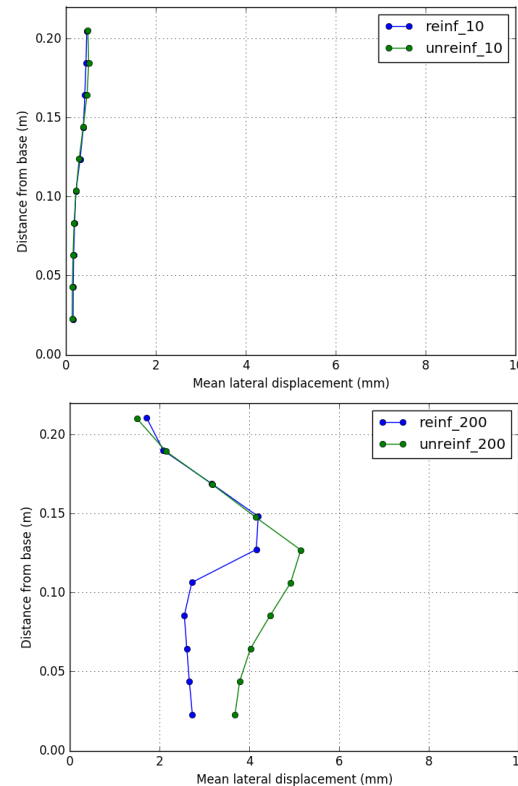
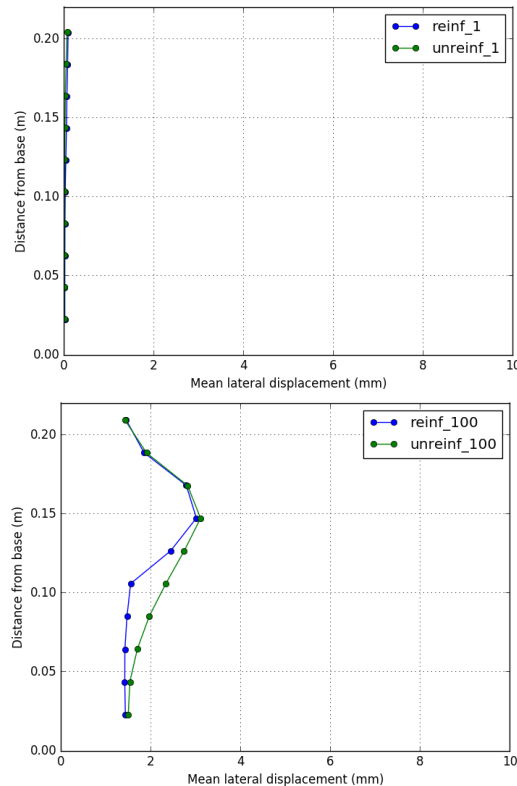


Stabilized- 25 mm GG, , 12.5 mm agg
Good interlocking



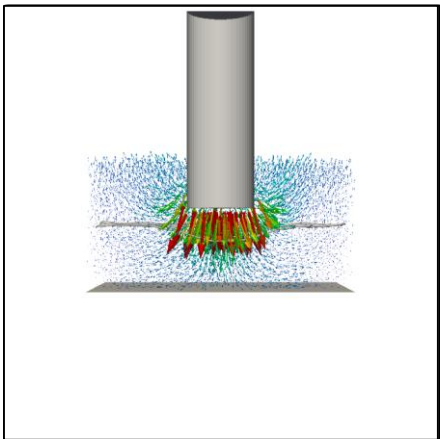
Stabilized- 12.5 mm GG, 15 mm agg
Insufficient interlocking

Geogrid Influence Zone – 37 mm GG

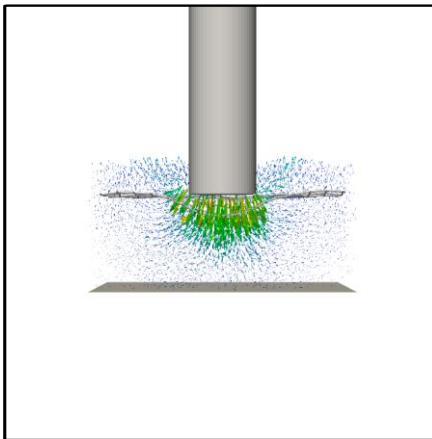


Comparison of mean lateral displacement profiles for Unstabilized and 37 mm geogrid

Effect of GG Location: H/2 vs H/3 [25 mm GG, 190 kPa]

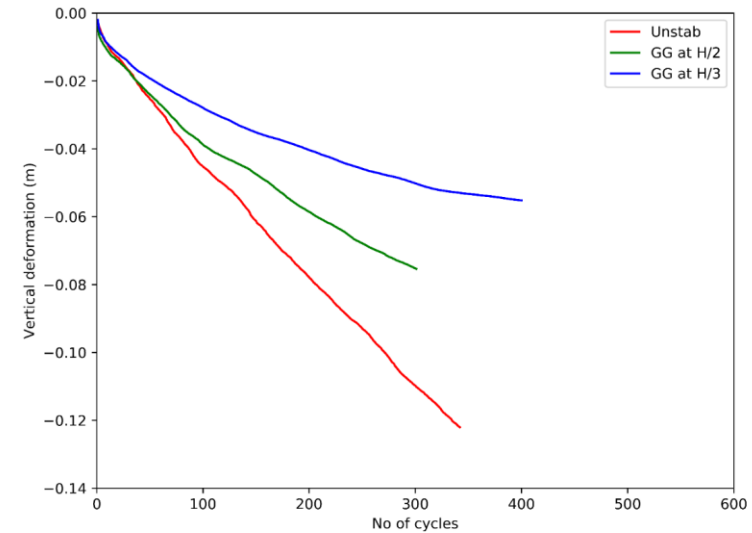


Stabilized- 25 mm GG
GG location = H/2 from base



Stabilized- 25 mm GG
GG location = H/3 from base

Cycle 300

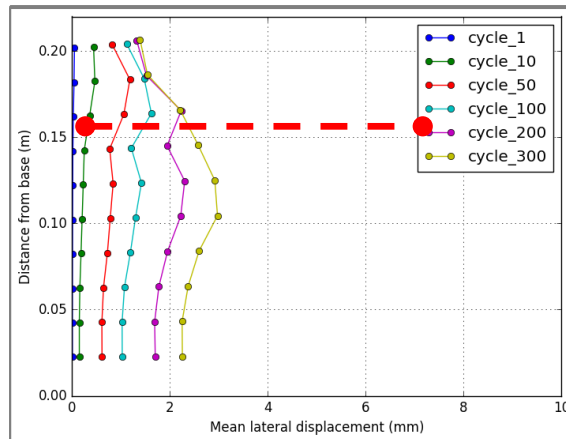
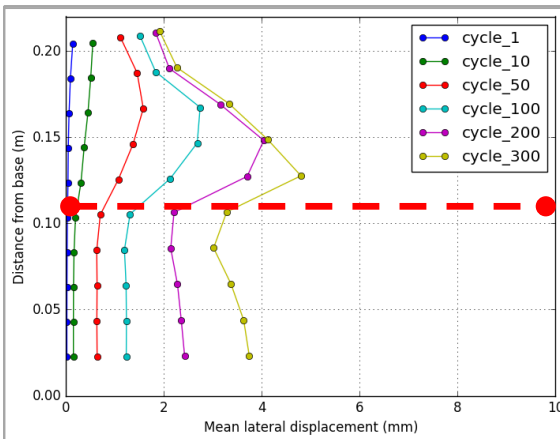
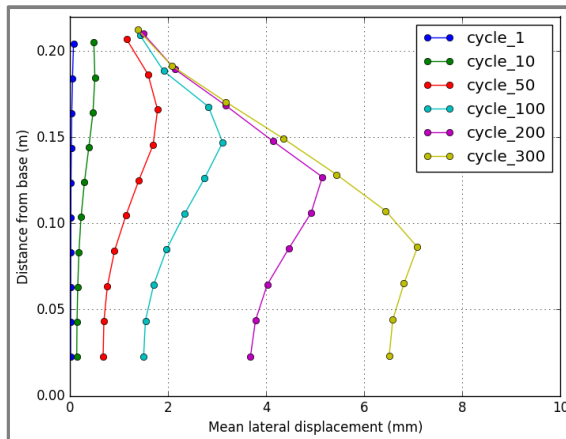


Surface rutting curves for various geogrid locations

Observations

- GG at 0.3 H limits exaggerated vertical deformations
- Also prevents early-stage accumulation of deformations (since it is closer to surface). Evident in rutting curves which shows early deviation from unstabilized curve

Lateral Disp Profiles : Unstabilized & GG @ H/2,GG @ H/3 [190 kPa, 25 mm GG]



Unstabilized
GG location = NA

Stabilized
GG location = 116 mm from base

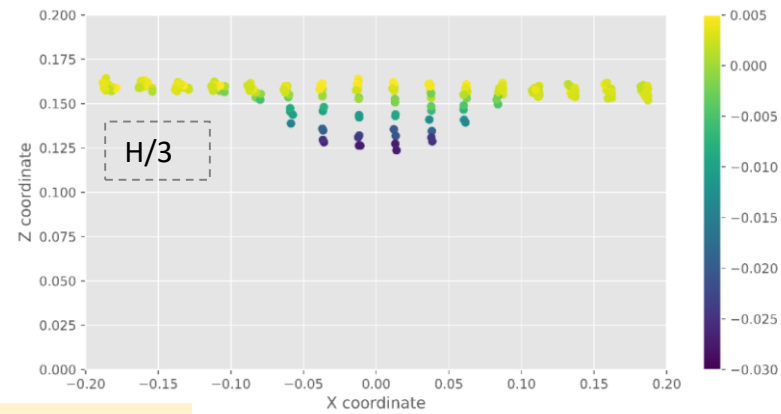
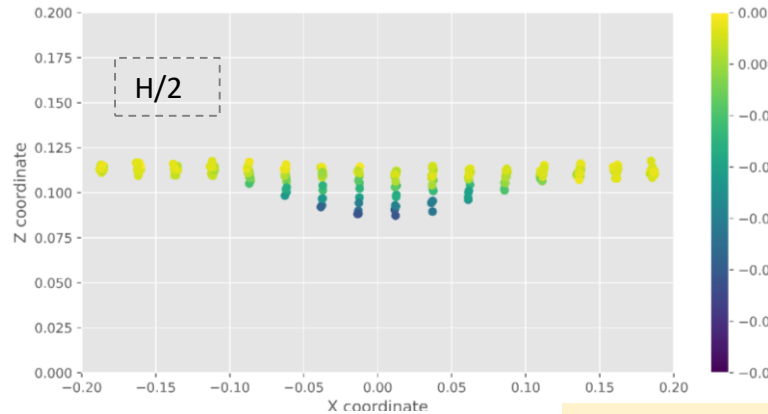
Stabilized
GG location = 163 mm from base

Profiles of **mean lateral displacement** across thickness of aggregate layer at different GG locations

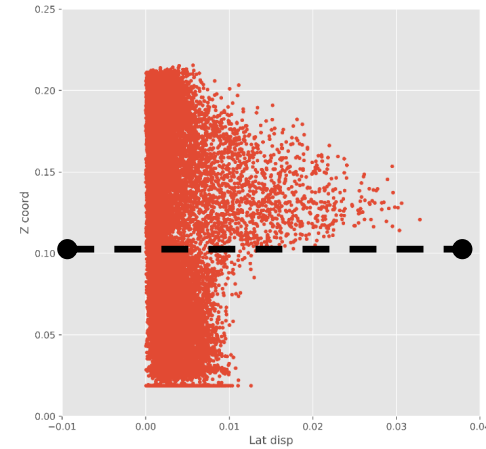
Observations

- GG at 0.3 H limits exaggerated vertical deformations + lateral displacements

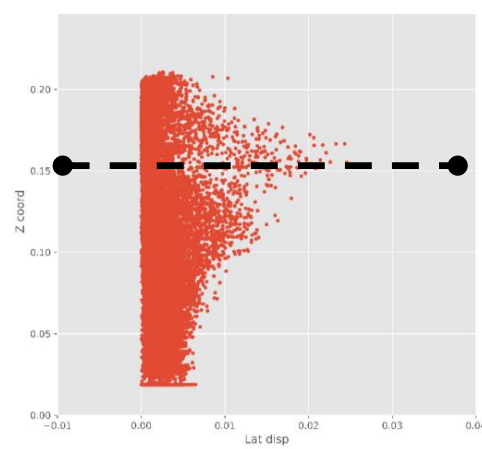
Geogrid location: H/2 vs H/3 [190 kPa, 25 mm GG]



GG node vertical displacement at
300 loading cycles



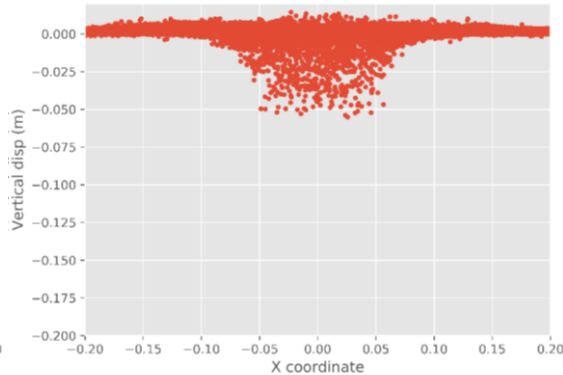
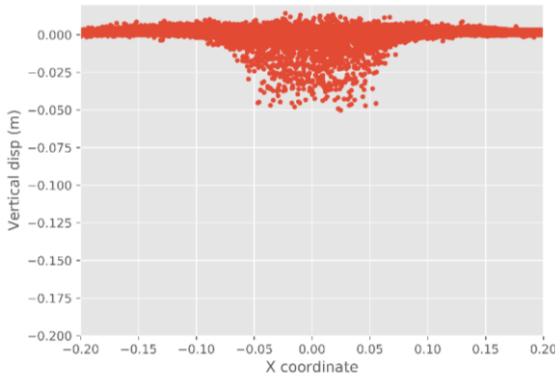
Lateral spreading at 300 cycles



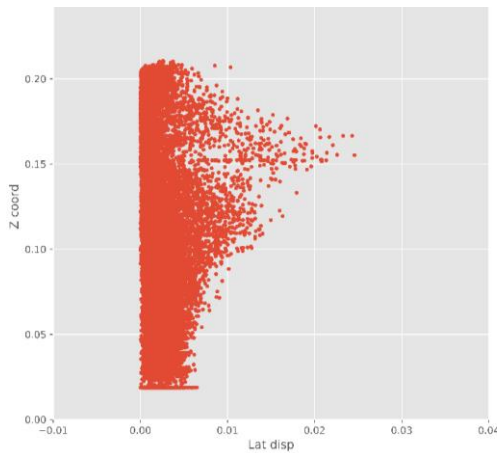
Geogrid location: H/3 [190 kPa, 25 mm GG] at 400 cycles

Observations

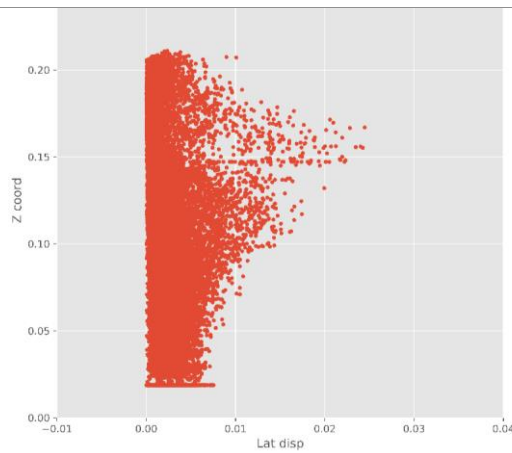
- Additional deformation of 0.005 m from 300 cycles
- Indicates stabilization



Comparison of vertical and lateral displacements at 300 and 400 cycles



300 cycles



400 cycles

Ongoing Work

- Incorporating rolling resistance to simulate angularity and study how aggregate-aggregate interlocking supplements geogrid-aggregate interlocking
- Perform simulations to study geogrid stiffness effect (steel vs geogrid)

Thank you

Please email me if you need any clarifications

References

- Al-Qadi, I.L. & Dessouky, S.H. & Kwon, J. & Tutumleur, E., 2008. Geogrid in Flexible Pavements: Validated Mechanism, *Transportation Research Record: Journal of the Transportation Research Board*, No 2045, 102-109.
- Barksdale, R.D. & Itani, S.Y., 1989. Influence of aggregate shape on base behavior, *Transportation Research Record: Journal of the Transportation Research Board*, No 1227, 173-182.
- Barksdale, R.D. & Brown, S.F. & Chan, F., 1989. Potential Benefits of Geosynthetics in Flexible Pavement Systems, *NCHRP Report 315, Transportation Research Board, Washington, D.C.*
- Brown, S.F. & Kwan, J. & Thom, N.H., 2007. Identifying the key parameters that influence geogrid reinforcement of railway ballast, *Geotextiles and Geomembranes*, 25, 326-335.
- Giroud, J.P., Ah-Line, C., and Bonaparte, R. Design of unpaved roads and trafficked areas with geogrids. Polymer grid reinforcement, 1985. 116–127.
- Giroud, J.P. & Han, J., 2004. Design Method for Geogrid-Reinforce Unpaved Roads: Development of Design Method, *Journal of Geotechnical and Geoenvironmental Engineering*, Vol. 130, 775-786.
- Jang, D. J., 1997. Quantification of sand structure and its evolution during shearing using image analysis, *PhD Thesis*, Georgia Institute of Technology, Atlanta.
- Kim, T. & Tutumleur, E., 2005. Unbound Aggregate Rutting Models for Stress Rotations and Effects of Moving Wheel Loads, *Transportation Research Record: Journal of the Transportation Research Board*, No 1913, 41-49.
- Kwon, J. & Boudreau, R.L. & Tutumleur, E. & Wayne, M.H., 2014. Evaluation and Characterization of Aggregates for Sustainable Use in Pavement Engineering, *ASCE Geo-Congress*, 3373-3382.
- Kwon, J. & Kim, S. & Tutumleur, E. & Wayne, M.H., 2017. Characterization of Unbound Aggregate Materials considering physical and morphological properties, *International Journal of Pavement Engineering*, 18:4, 303-308.
- Mishra, D. & Tutumleur, E., 2012. Aggregate Physical Properties Affecting Modulus and Deformation Characteristics of Unsurfaced Pavements, *Journal of Materials in Civil Engineering*, 24(9), 1144-1152.
- Monismith, C.L. & Ogawa, N. & Freeme, C.R., 1985. Permanent Deformation Characteristics of Subgrade Soils due to Repeated Loading, *Transportation Research Record: Journal of the Transportation Research Board*, No 537, 1-17.
- Thompson, M.R., 1998. State of the Art: Unbound base performance, *Proceedings of the Sixth Annual Symposium of International Center for Aggregate Research (ICAR), Austin, TX*.
- Archer, S. & Wayne. M.H., 2012. Relevancy of Material Properties in Predicting the Performance of Geogrid-Reinforced Roadways, *ASCE Geo-Congress*, 1320-1329
- Tseng, K.H. & Lytton, R.L., 1989. Prediction of Permanent Deformation in Flexible Pavement Materials, *ASTM STP*, 1016, 154-172
- Xiao, Y., Tutumleur, E. & Qian, Y. & Siekmeier, J.A., 2012. Gradation Effects Influencing Mechanical Properties of Aggregate Base-Granular Subbase Materials in Minnesota, *Transportation Research Record: Journal of the Transportation Research Board*, No 2267, 14-26.
- Vangla, P., Roy, N., & Gali, M. L. (2018). Image based shape characterization of granular materials and its effect on kinematics of particle motion. *Granular Matter*, 20(1), 6.
- Zornberg, J.G., 2011. Advances in the Use of Geosynthetic in Pavement Design, *Proceedings of the Second National Conference on Geosynthetics, Geosynthetics India '11, Vol 1*, 3-21.